Photoelectron spectroscopy of strongly correlated systems: Effects of nonlocal interactions

Jianzhong Zheng and Changfeng Chen
Department of Physics, University of Nevada, Las Vegas, Nevada 89154
(Received 16 January 1995)

We present a theoretical description of the one-particle excitation spectra in strongly correlated systems with nonlocal interactions. Using exact diagonalization techniques, photoemission and inverse photoemission spectra of an extended Hubbard model with an intersite Coulomb interaction are calculated. The single-particle and many-body aspects are treated on an equal footing. The hopping and interaction parameters are adjusted to simulate various Hubbard and charge-transfer systems. In contrast to normal expectations, the intersite interaction is found to suppress the spectral features driven by the on-site interaction, leading to a narrowing in the overall spectral distribution. It also produces qualitatively new behavior in the spin polarization of the spectra and in the doping dependence of the low-energy spectral weight. The degree of sensitivity of the spectra to the single-particle and interaction parameters is systematically investigated. General implications of the calculated results for strongly correlated systems are discussed.

I. INTRODUCTION

Photoelectron spectroscopy provides a direct measurement of the fermion excitations in electron systems.[1] The energy and angle (momentum) resolutions of photoemission experiments have been improved significantly over the last few years, largely driven by intensive studies of the high-temperature superconductors and other strongly correlated electron systems.[2] Combined with spin-polarized detection capability, this technique is able to reveal very detailed features in electronic structures of materials systems. From a theoretical point of view, the challenge is to determine the electronic energy spectrum or the density of states (DOS) of the system.[3] In the weak-interaction limit, photoelectron spectra essentially map out the electronic DOS of the system, which can be directly compared with the results of single-particle theories with local-density approximations (LDA). However, when interactions are strong the concept of single-particle DOS becomes ill-defined. It is more appropriate to study one-particle excitation spectra that depend sensitively on the interactions. In general, the interaction-induced electron correlations cause nontrivial transfer of spectral weight. In this situation a many-body calculation and a thoughtful interpretation of the results are of crucial importance for the understanding of the observed phenomena and the underlying physics. Most theoretical work in this field has focused on relatively "simple" models such as the Hubbard model and the t-J model, with the expectation of capturing the fundamental physics underlying the observed new phenomena. Significant progress along this line has been made in recent years.[4]

The key issue in the study of photoelectron spectra of strongly correlated electron systems is the role of the interactions in determining the spectral weight distribution. Extensive earlier experimental[5] and theoretical[6] work has established that the strong Coulomb interactions (mainly on-site, such as the U term in the ordinary Hubbard model) drive the spectral weight from a "coherent" to an "incoherent" part, yielding new spectral features beyond the energy range predicted by single-particle theories, and therefore a *broadened overall spectral distribution*, along with a reduction in the bandwidth and the exchange splitting in the low-energy-scale and an increase in the exchange splitting and spin polarization on the high-energy side of the spectrum. The physical insights gained from the studies of the Hubbard model and its variants are extremely helpful in interpreting the results and extracting the relevant physics from experiments and more realistic calculations.[7]

In this paper we investigate the spectral behavior of strongly correlated systems with nonlocal interactions. We study an extended Hubbard model with intersite interactions. Various parameter choices corresponding to different physical systems have been used to study the dependence of the spectral distribution on the nonlocal interactions. Some interesting results, including an intersite-interaction-driven *overall spectral narrowing* and anomalous behavior in the spin polarization of the spectra and in the doping dependence of the low-energy spectral weight, have been observed in the calculated results. These results are analyzed in a many-body picture and are expected to have general implications for a wide variety of strongly correlated systems.

We employ a symmetry-projected exact-diagonalization approach to study the many-body Hamiltonian defined on a small cluster with periodic boundary conditions. This approach has proven to be very good at treating strongly correlated systems. It is particularly useful in interpreting and predicting qualitative behavior produced by strong interactions. Combined with other theoretical approaches, such as the real-space density-matrix renormalization-group approach[8] and the band-structure calculation method,[7] the exact-diagonalization approach can provide accurate quantitative and material-specific

0163-1829/95/51(20)/14092(11)/$06.00

results for strongly correlated systems. In addition to using particle-number and spin symmetries to block diagonalize the Hamiltonian matrix, group theoretical techniques have been applied to project out symmetrized states according to the spatial symmetry of the system.[9] The full utilization of these symmetries has greatly facilitated the numerical computation of the spectra.

The rest of this paper is organized as follows. In Sec. II we introduce the model Hamiltonian and discuss the related theoretical and computational issues. In Sec. III, the calculated results are presented and analyzed in a many-body picture. Finally, conclusions are given in Sec. IV.

II. THEORETICAL AND COMPUTATIONAL ASPECTS

A. The Model Hamiltonian

We define an extended Hubbard model with the following model Hamiltonian:

$$H = \sum_{i,j;\sigma} t_{ij} c^{\dagger}_{i\sigma} c_{j\sigma} + (1/2) \sum_{i;\sigma} U_i n_{i\sigma} n_{i-\sigma} + \sum_{i<j} K_{ij} n_i n_j, \quad (1)$$

where t_{ij} is the hopping parameter, $n_i = \sum_{\sigma} n_{i\sigma}$, and U_i (K_{ij}) is the on-site (intersite) Coulomb interaction parameter. We consider the first and second nearest-neighbor hopping with amplitude $-t$ and $-s$, respectively. The on-site Coulomb interaction is assumed to be the same on all sites in the ordinary Hubbard model and assigned differently (to be specified below) in the charge-transfer model. We consider only the intersite interaction K between the nearest-neighbor sites, which is the dominant off-site term. All the calculations reported in this work have seven or six electrons (or equivalently one-hole or two-hole doped) in the cluster, i.e., a system with an almost half-filled band.

The Hamiltonian (1) is defined on an eight-site cluster with periodic boundary conditions as shown in Fig. 1(a). With proper assignments of "d" and "p" orbitals, this structure is equivalent to a Cu_4O_8 cluster which was studied as representing the CuO_2 planes in the high-T_c superconductors.[10] It is also equivalent to a periodic cluster with two-orbital unit cells which was used in the study of transfer of spectral weight in correlated systems.[11] In this work we first consider a uniform Hubbard system and then a two-sublattice charge-transfer system with the focus on the effect of the intersite interaction in both cases. We emphasize the generic properties of the system that are qualitatively independent of the system size and structure as well as dimensionality. It has been observed previously that generic spectral features of the Hubbard model are indeed essentially independent of the system structure and size for clusters as small as only eight sites.[11,12]

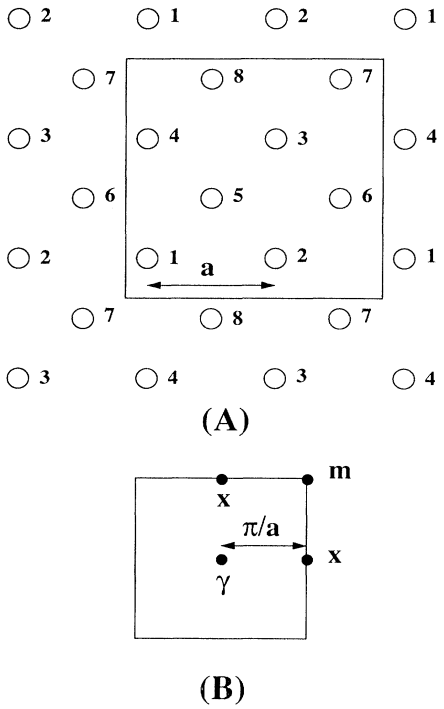

FIG. 1. (a) The eight-site cluster with periodic boundary conditions in real space. The lattice constant is a. (b) the two-dimensional Brillouin zone with the four sampled high-symmetry points indicated.

B. Method of calculation

The theoretical method used in this work is the small-cluster approach.[9] A cluster of a small number of lattice sites with periodic boundary conditions is used to model an infinite system. It is equivalent to sampling a few high-symmetry points in the Brillouin zone. This method has been widely used in the study of strongly correlated systems. Its advantage is that there is no approximation applied to the Hamiltonian. Quantum many-body problems are solved *exactly* in the numerical form. Therefore it provides accurate information about the many-body effect in the system. Its limitation is also obvious. Due to extremely rapid growth of the number of many-body states with the system size and particle number, only very small systems can be studied using this approach. In practice, since many spectroscopic processes are fast and intrinsically short-ranged they can be well described by the small-cluster approach. Numerous work on this subject has been reported. It is now generally accepted that the sudden (one-step) approximation and small-cluster approach provide rather accurate description of many interacting systems, although careful modeling and insightful interpretation of the calculated results are always required.

With two (one for each spin) orbitals on each site, there are 16 orbitals in the cluster shown in Fig. 1(a). Simple combinatorial arguments yield 11 440 many-body states

in the neutral state of the cluster with seven electrons. Photoemission (inverse photoemission) process destroys (creates) an electron in the cluster, yielding 8008 (12 870) final states. The symmetries inherent in the Hamiltonian must be exploited in order to diagonalize the complete many-body Hamiltonian matrices. First, the total number of electrons in the cluster is a good quantum number. It ensures that there will be no mixing between states with a different number of electrons. Total spin and its z component in the cluster also are good quantum numbers. Spin operators are applied to sort out states with definite spin indices. Furthermore, space-group decomposition reduces the sizes of Hamiltonian matrices in a very efficient way, as will be described below.

The cluster studied in this work has C_4 point-group symmetry. The space group of the system with the periodic boundary condition is the direct product of the C_4 group and the finite translational group of the periodic-cluster structure which, in the present case, is a four-element group, consisting of the identical translation and the translations that connect a site, say site 1, in the cluster to the other three sites, sites 2, 3, and 4, on the square lattice. The vectors that connect site 1 to sites 5–8 are not included because in the charge-transfer model sites 1–4 and sites 5–8 are assumed to be different. This symmetry arrangement corresponds to sampling the γ point, the center of the two-dimensional Brillouin zone, the m point, the corner of the zone boundary, and the x point, the center of the zone boundary [see Fig. 1(b)]. The space group consists of 16 operations that belong to ten classes. There are ten irreducible representations, four at γ ($\gamma_1-\gamma_4$), four at m (m_1-m_4), and two at x (x_1 and x_2). The first eight representations are one-dimensional and the last two are two-dimensional. Two pairs of representations, m_1-m_2 and m_3-m_4, are degenerate due to time-reversal symmetry. The character table is given in Table I. With a complete set of matrices that transform according to the irreducible representations, it is possible to project out sets of symmetrized basis states,

$$\Psi^j_{\mu S}=\sum_R \chi^\mu_R P_R \psi^j_S, \tag{2}$$

where ψ^j_S is the jth state in the subspace of spin S (S may describe *both* the total and z component of spin), P_R is the projection operator corresponding to the space-group element R, χ^μ_R is the corresponding character, and $\Psi^j_{\mu S}$ is the symmetrized basis state with definite spin S and spatial symmetry μ. In cases where the irreducible representations are not one-dimensional, the (1×1) element of the matrix representation is used to project out the symmetrized states as the basis set. The partner states, which are not needed in the diagonalization of the Hamiltonian matrices but are necessary for the calculation of the spectra, can be obtained by applying to the above states the projection operator[13]

$$\mathcal{P}^p_{mn}=(d_p/g)\sum_R \Gamma^p(R)^*_{mn}P_R, \tag{3}$$

where d_p is the dimension of the pth irreducible representation, g is the order of the space group, and $\Gamma^p(R)^*_{mn}$ is the complex conjugate of the mn element of the matrix representation of the pth irreducible representation for the operation element R. By setting $n=1$ and varying m (>1) in Eq. (3), one can project out all d_p states that transform according to Γ^p.

Once the index j in Eq. (2) runs through the whole subspace with a fixed number of particles and definite spin index, all the symmetrized states are sorted and properly normalized. This procedure is repeated for all subspaces involved in a given physical process. Since group theory guarantees[13] that Hamiltonian matrix elements between states belonging to different irreducible representations are always zero, the original Hamiltonian matrix is now decomposed into smaller Jordan blocks with distinct particle-number, spin, and spatial symmetries. The largest block is of order 296 corresponding to eight electrons in the cluster with a total spin $S=1$. It is significantly smaller than the original Hamiltonian matrix of order 12 870, which in turn drastically reduces the required computation time. The solutions obtained by diagonalizing these blocks are exact solutions of the full Hamiltonian for the cluster.

In the computational implementation of the projec-

TABLE I. The character table of the space group for the cluster with periodic boundary conditions studied in this work [see Fig. 1(a)]. The point group of the cluster structures is of C_4 symmetry. There are four elements in the translational group: the identical translation t_0 and the translations t_1, t_2, and t_3 that connect a site, say site 1, to the other three sites that share the same square, i.e., sites 2, 4, and 3, respectively.

	E	C_4^2	$\{E\|t_3\}$	$\{C_4^2\|t_3\}$	$\{E\|t_1\}$ $\{E\|t_2\}$	$\{C_4^2\|t_1\}$ $\{C_4^2\|t_2\}$	$\{C_4\|t_1\}$ $\{C_4\|t_2\}$	$\{C_4^{-1}\|t_1\}$ $\{C_4^{-1}\|t_2\}$	C_4 $\{C_4\|t_3\}$	C_4^{-1} $\{C_4^{-1}\|t_3\}$
γ_1	1	1	1	1	1	1	1	1	1	1
γ_2	1	1	1	1	1	1	−1	−1	−1	−1
γ_3	1	1	1	1	−1	−1	−1	−1	1	1
γ_4	1	1	1	1	−1	−1	1	1	−1	−1
m_1	1	−1	1	−1	1	−1	i	$-i$	i	$-i$
m_2	1	−1	1	−1	1	−1	$-i$	i	$-i$	i
m_3	1	−1	1	−1	−1	1	i	$-i$	$-i$	i
m_4	1	−1	1	−1	−1	1	$-i$	i	i	$-i$
x_1	2	−2	−2	2	0	0	0	0	0	0
x_2	2	2	−2	−2	0	0	0	0	0	0

tion of symmetrized states, we used a real-number-only algorithm for the convenience of coding. Since there are imaginary numbers involved in the character table (see Table I), linear combinations of the projection operators of the degenerate irreducible representations (i.e., m_1-m_2 and m_3-m_4 pairs) are taken so that all characters used in the codes are real integers. The price for so doing is the doubling of the size of the matrix blocks for the representations involved. When dealing with larger matrices the codes can be modified to release this real-number-only restriction, thus avoiding the accompanied increase in the size of the Hamiltonian matrix.

C. Calculation of the spectra

With all the eigenvalues and eigenstates of the system obtained through the exact diagonalization of the Hamiltonian matrix, we can calculate any correlation function of interest in the context of the small-cluster approach. In this work we focus on the effects of the nonlocal interaction on the photoelectron spectral distribution. The spin-resolved photoemission spectrum (PES) and inverse photoemission spectrum (IPES) are defined as

$$F_{\rm PES}(\omega,\sigma)=\sum_{n,k}|\langle\phi_n^{N-1}|c_{k,\sigma}|\phi_0\rangle|^2 \times\delta(\omega+E_n^{N-1}-E_0^N+\mu), \quad (4)$$

$$F_{\rm IPES}(\omega,\sigma)=\sum_{n,k}|\langle\phi_n^{N+1}|c_{k,\sigma}^\dagger|\phi_0\rangle|^2 \times\delta(\omega-E_n^{N+1}+E_0^N+\mu), \quad (5)$$

where $|\phi_0\rangle$ is the ground state in the subspace of N electrons with energy E_0^N, and $|\phi_n^{N\pm1}\rangle$ are eigenstates in the subspace of $N\pm1$ electrons with energies $E_n^{N\pm1}$. The operator $c_{k,\sigma}$ ($c_{k,\sigma}^\dagger$) destroys (creates) an electron with spin σ and composite index k, where k may include orbital and momentum indices. The chemical potential μ is determined from[14]

$$\mu=(1/2)[E_0^{N+1}-E_0^{N-1}]. \quad (6)$$

In several reported cases, the ground state of the system is degenerate. In such situations, the spectra are calculated with each and every state in the ground-state manifold as the ground state, and the final results are obtained by averaging over the spectra contributed by all the states in the manifold. The discrete spikes in the calculated spectra, which are characteristic of small-cluster calculations, are broadened with Gaussian functions so that the fine spectral structures that depend on the details of the cluster size and structure are smoothed out. We shall focus attention here on the general trend that is independent of such details. The calculated results are checked against the following sum rules:

$$\int F_{\rm PES}(\omega,\sigma)d\omega=N_\sigma, \quad (7)$$

$$\int F_{\rm IPES}(\omega,\sigma)d\omega=M-N_\sigma, \quad (8)$$

where M is the total number of sites in the cluster and N_σ is the total number of electrons with spin σ in the ground state of the N-electron system. These sum rules are satisfied in all the reported cases.

It is usually expected that interactions will result in a broadening in the spectral distribution. The origin of the spectral broadening is that the states $c_{k,\sigma}|\phi_0\rangle$ and $c_{k,\sigma}^\dagger|\phi_0\rangle$ obtained by sudden annihilation and creation of an electron in the ground state of the N-electron system are not exact eigenstates of the interacting system with $N\pm1$ electrons. Decomposed in a complete basis of eigenstates they have projections in virtually *all of the final states* with the same quantum numbers. As a result, a certain portion (usually of high spin polarization) of the spectral weight will be transferred to the high-energy scale, creating the so-called "incoherent" part, or "satellite peak," and causing a broadening in the spectral distribution.

For a better understanding of the physics involved in the context of the exact diagonalization study of finite systems, we examine in more detail the spectral function in a many-body picture. Consider the photoemission case and assume that $\{\psi_l^N, l=1,2,...\}$ and $\{\psi_j^{N-1}, j=1,2,...\}$ are the symmetrized complete basis sets used in the construction of the Hamiltonian matrices for the N- and $(N-1)$-electron system, with corresponding energy spectrum (eigenvalues) $\{\varepsilon_l^N\}$ and $\{\varepsilon_j^{N-1}\}$, respectively. Configurational interactions mix virtually all the states with the same quantum numbers. Consequently the N-electron ground state and the $(N-1)$-electron final states, with energies E_0^N and E_n^{N-1}, respectively, can be expressed as

$$|\phi_0^N\rangle=\sum_l\alpha_l^{(0)}\psi_l^N, \quad (9)$$

$$|\phi_n^{N-1}\rangle=\sum_j\beta_j^{(n)}\psi_j^{N-1}, \quad (10)$$

where $\alpha_l^{(0)}$ and $\beta_j^{(n)}$ are the corresponding coefficients. The PES defined in Eq. (4) now reads

$$F_{\rm PES}(\omega,\sigma)=\sum_{n,\gamma}\left|\sum_{l,j}\alpha_l^{(0)}\beta_j^{(n)}\langle\psi_j^{N-1}|c_{\gamma,\sigma}|\psi_l^N\rangle\right|^2 \times\delta(\omega+E_n^{N-1}-E_0^N+\mu). \quad (11)$$

It is clear that by destroying an electron in the ground state and then mapping it onto the $(N-1)$-electron final states one is trying to match the set of states $\{c_{\gamma,\sigma}\psi_l^N\}$ to the set $\{\psi_j^{N-1}\}$. And the contribution of a "matched" term to the PES is determined by the product of the coefficients $\alpha_l^{(0)}$ and $\beta_j^{(n)}$. It is important to note that these coefficients depend very sensitively on the structure of

the energy (eigenvalue) spectrum. They decrease very rapidly with increasing energy. Therefore the spectral function corresponding to high-energy final states usually carries only negligible weight. The situation in the inverse photoemission spectra is similar.

III. RESULTS AND DISCUSSION

It is well established that the on-site interaction in the ordinary Hubbard model drives the spectral weight to higher energies and makes the spin polarization and the exchange splitting reduced at the low-energy scale and increased on the opposite side of the spectra. For the purpose of comparison, we have calculated the spectra for the Hamiltonian (1) with the intersite interaction $K = 0.0$, i.e., an ordinary Hubbard model. The nearest-neighbor hopping parameter t is chosen as the energy unit and the next-nearest-neighbor hopping parameter s is set to be 0.7. The PES and IPES with different values of U are calculated. For clarity of the presentation the results are plotted separately in Figs. 2 and 3. Several features that are characteristic of such systems are observed. It is clearly seen that the PES and IPES spectral distributions are broadened, as expected, with increasing U. An analysis of the spin-resolved spectra reveals that as the interaction strength grows the spin polarization is reduced at the low-energy scale and enhanced at the high-energy scale. This behavior is well understood as the result of the reduced probability of finding two particles of opposite spin orientations in and near the ground state of the system.[6,7] In the $U = 10$ case, distinct satellite peaks have developed in both the PES and the IPES with almost full spin polarization in majority- and minority-spin orientations, respectively.

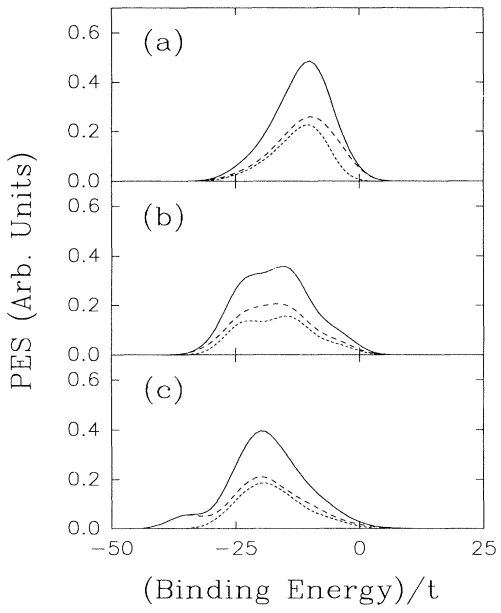

FIG. 2. The calculated photoemission spectrum (PES) with seven electrons in the ground state. The parameters are $t = 1.0$, $s = 0.7$, $K = 0.0$, and $U = 1.0$ (a), 5.0 (b), and 10.0 (c). The solid, long-, and short-dashed lines represent the total, majority-, and minority-spin results.

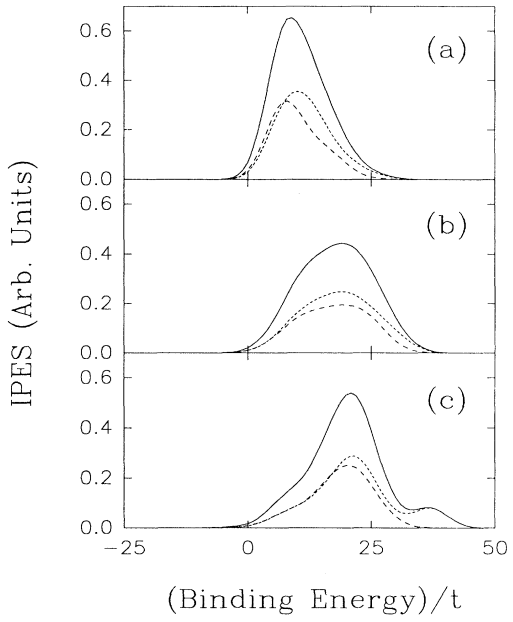

FIG. 3. The calculated inverse photoemission spectrum (IPES) with seven electrons in the ground state. The parameters are the same as in Fig. 2.

Normally additional interactions are expected to further drive spectral weight toward the high-energy scale, leading to an even broader overall spectral distribution, and strengthen the effects on the spin polarization of the spectra. In Fig. 4 we show the calculated PES for $U = 5.0$ and various nonzero values of K [for the K=0 result, see Fig. 2(b)]. It immediately catches the attention that there is a K-driven *narrowing* instead of a broadening in the overall spectral distribution. In addition, the spin polarization of the spectrum shows anomalous behavior. It is first reduced on the low-energy scale and enhanced on the high-energy scale, similar to the situation one would expect for an ordinary Hubbard system. However, when the intersite term increases further, the spin polarization starts to grow on the low-energy scale and decrease on the high-energy scale. This cannot be explained by the picture proposed above for the ordinary Hubbard model.

To explain these anomalous features we examine in more detail the spectral function in a many-body picture. We analyze the qualitative physics by using a simple system, a dimer with two electrons in the atomic limit. When $K = 0$, the energy of the system is $E_0 = 0$ for the configuration with two singly occupied sites and $E_1 = U$ for the configuration with a doubly occupied site. One expects to observe spectral weight at these energies separated by $\Delta = U$. When K is turned on, one

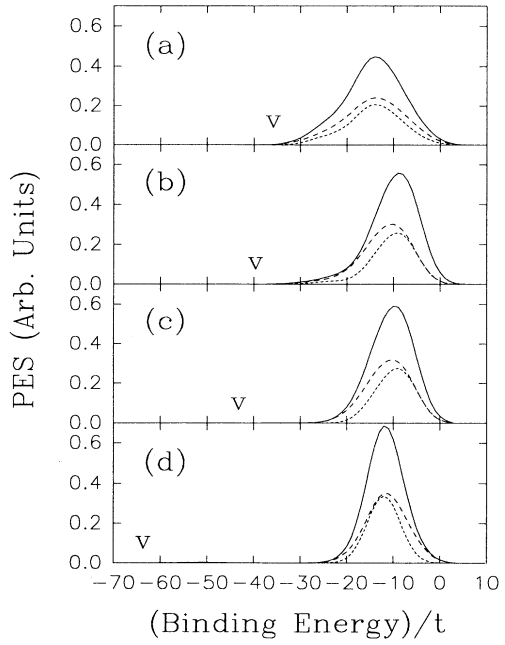

FIG. 4. The calculated photoemission spectrum (PES) with seven electrons in the ground state. The parameters are $t = 1.0$, $s = 0.7$, $U = 5.0$, and $K = 1.0$ (a), 3.0 (b), 5.0 (c), and 9.0 (d). The solid, long-, and short-dashed lines represent the total, majority-, and minority-spin results. The tip of the letter "V" indicates the highest energy position of the spectral distribution (see the text for more details).

has $E_0 = K$, $E_1 = U$, and $\Delta = U - K$. It is seen that Δ decreases with increasing K. Therefore, the increasing intersite interaction results in a narrower spectral distribution in the photoemission spectrum. This picture is qualitatively applicable to all strongly correlated systems with different filling factors, larger sizes, and more complex structures.

Guided by this simple picture we can easily understand the quantitative results presented in Fig. 4. We have compared the spectrum calculated with the interaction parameters $K = 0.0$ and $U = 5.0$ with the single-particle (i.e., $K = 0.0$ and $U = 0.0$) electronic structure of the same model. A detailed analysis of the calculated data identifies that the high-energy spectral weight beyond $-25t$ in Fig. 2(b) is driven by the on-site interaction U; there is also a significant amount of spectral weight transferred from the low-energy region to the energy range between $-20t$ to $-25t$ due to the U term. The intersite interaction is found to gradually push the spectral weight toward the low-energy scale as expected, yielding the observed spectral narrowing [Figs. 4(a)–4(d)].

When the intersite interaction K is large enough, it drives electrons into paired states (since Δ becomes negative). A representative configuration in the ground state of the present system with large K has the sites 1, 2, and 3 doubly occupied and the site 4 singly occupied (see Fig. 1 for the cluster structure). This configuration is energetically favorable since the nearest-neighbor interaction K is avoided. In this situation, the photoemission spectrum becomes essentially K-independent. We have calculated the PES for $K = 15.0$. The results are indeed almost identical to that shown in Fig. 4(d) with $K = 9.0$.

The above simple picture also explains the anomalous spin polarization observed in the calculated spectra. When K is initially turned on, the spectral weight corresponding to the configurations with doubly occupied sites is pushed toward the low-energy scale. As a result, the spectral distribution narrows and the spin polarization increases slightly at low energies [see Figs. 2(b) and 4(a)]. As the K increases further, the competition between the U and the K term, with the latter enhancing (reducing) the spin polarization in the high (low) -energy scale, produces an almost spin-neutral low-energy spectrum and a highly polarized high-energy spectrum [see Figs. 4(b) and 4(c)]. Finally, when the K term becomes dominant (but its *direct* contribution to the total energy is avoided in the ground-state configuration), the paired configurations become energetically favorable and, therefore, *the U-driven effects manifest themselves in the low-energy scale of the spectrum.* It reverses the situation in the ordinary Hubbard model and leads to an increase in the spin polarization and the exchange splitting in the low-energy scale [Fig. 4(d)]. The spectral weight near the chemical potential is now driven by the on-site interaction U and is transferred to higher energies. As a result the spectral distribution is further narrowed from the low-energy side due to the U term, in addition to the narrowing on the high-energy side due to the K term.

Although the intersite interaction causes significant spectral narrowing as presented above, it should be pointed out that, according to Eq. (11) and the discussion immediately below it, there should be spectral distribution at high energies corresponding to highly excited final states. By carefully examining the calculated numerical results, we indeed found spectral distribution at energies higher than the high-energy tail of the peak that is visible in the plotted figures. The highest energy position of such spectral distribution is indicated by the tip of the letter "V" in Fig. 4. It moves to higher energies as K increases. However, these high-energy spectra carry only negligible weight, as expected. It should be noted that the move of the highest-energy position simply reflects the expansion of the range of the energy spectrum of the system. It is not related to the anomalous spectral behavior presented above. The latter is a reflection of the nature of the many-body states, the ground state in particular, of the system in response to changes in the nonlocal interaction.

The inverse photoemission spectra with the same parameters as used in Fig. 4 are presented in Fig. 5. A K-driven spectral narrowing is clearly seen by comparing the $K = 0.0$ spectrum shown in Fig. 3(b) and the $K = 1.0$ spectrum in Fig. 5(a). It can be understood in the same physical picture as proposed for the PES.[16] As the value of K increases further, a low-energy peak develops while a larger peak is pushed to higher energies. The total integrated weight is found to be 1.0 for the low-energy peak and 8.0 for the high-energy peak. In addition, the low-energy peak is fully polarized in the

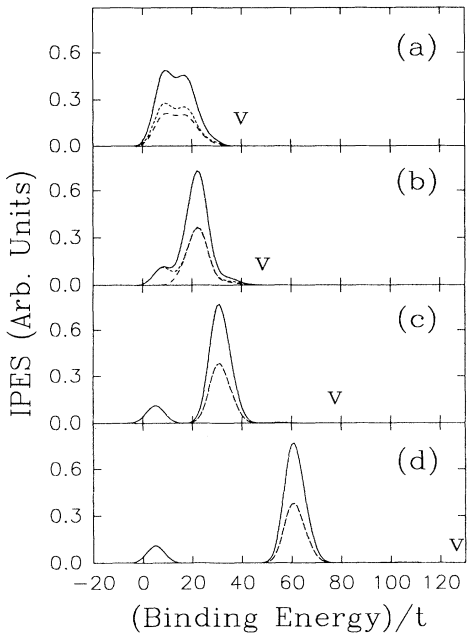

FIG. 5. The calculated inverse photoemission spectrum (IPES) with seven electrons in the ground state. The parameters are the same as in Fig. 4.

minority-spin orientation, while the high-energy peak is spin neutral. The energy separation between the two peaks grows with increasing K. These results also can be understood in the picture proposed above. For clarity, we again consider the large-K ground-state configuration presented above with the sites 1, 2, and 3 doubly occupied and the site 4 singly occupied. The unpaired electron is in the majority-spin state since the calculated ground state has a total spin of $S = \frac{1}{2}$. The additional electron introduced by the IPES process may occupy the *minority-spin* state on the singly occupied site, with an energy increase of U, or it may occupy one of the empty sites 5–8, with an equal probability on orbitals of either spin orientation with an energy increment of $7K$. The ratio of the configurational space available for these two processes is 1:8. The energy separation between the two peaks is $7K-U$. These results are in excellent agreement with the calculated IPES shown in Fig. 5. Similar to the situation in the PES shown in Fig. 4, spectral distribution with negligible weights is found at higher energies with the highest-energy position indicated by the tip of the letter "V."

It is interesting to note that the above results suggest an unusual doping dependence of the low-energy spectral weight that is proportional to the hole concentration x when the system is doped away from half-filling. This is quite different from the results for the ordinary Hubbard model, where, as proposed by Sawatzky and coworkers,[11,15] the doping dependence is $2x$ or even faster. The linear relation in the present case is actually the same as that in a semiconductor. However, there is a distinct difference here. In semiconductors, the low-energy peak is expected to be spin neutral. In the present case, it is fully polarized due to the intersite interaction as explained above. It should be noted, however, that when the system is further doped away from half-filling the situation is quite different in regard to the spin polarization of the low-energy peak in the IPES. We have calculated the PES and IPES of the same model with identical Hamiltonian parameters but with six electrons in the ground state of the system. The results are shown in Figs. 6 and 7. It is seen that almost all the spectral features presented above for seven electrons in the cluster are reproduced qualitatively, which can be explained in the same physical picture. The only exception is that the low-energy peak in IPES, which now carries $\frac{1}{4}$ of the total spectral weight (i.e., still linearly proportional to the hole concentration x), is *spin neutral*. This is because the six-electron ground state has a total spin $S=0$, thus providing equal configurational space for the up and down spin states of the additional electron introduced by the inverse photoemission process. This indicates the possibility of observing in some systems with moderate to large nonlocal interactions a low-energy peak in IPES that has the spectral weight growing linearly with the doping concentration and the spin polarization developing from fully polarized to neutral as the system is doped away from half-filling. Therefore, *a correlated system with large nonlocal interactions behaves quite differently from either a semiconductor or a system described by the ordinary Hubbard model with respect to doping.*

We have calculated PES and IPES for a different set of parameters to test the sensitivity of the spectra to the single-particle electronic structure of the system. We turned off the second nearest-neighbor hoppings (i.e., set $s = 0$) and kept the other parameters the same as used in Fig. 4. It is found that the calculated spectral features are essentially identical, except for some slight quantitative changes, to the results presented above. In other words, the spectral features reported above are a rather general property of the interacting electron sys-

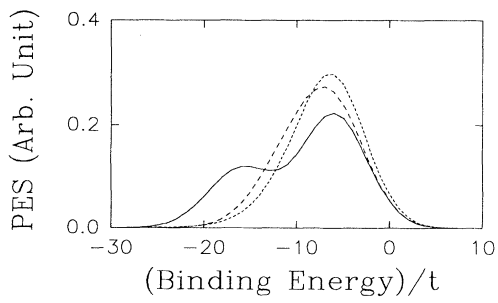

FIG. 6. The calculated photoemission spectrum (PES) with six electrons in the ground state. The parameters are the same as in Fig. 4, except that here the spectra for $K =$ 0.0 (solid line), 1.0 (long-dashed line), and 5.0 (short-dashed line) are presented. The ground state has a total spin $S = 0$. As a result all the spectra are spin neutral.

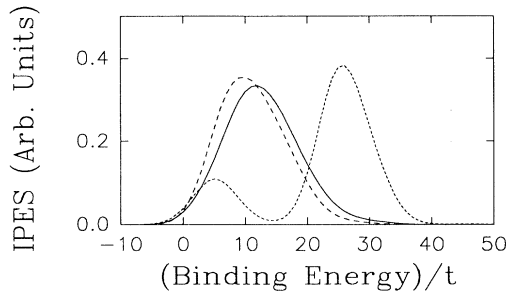

FIG. 7. The calculated inverse photoemission spectrum (IPES) with six electrons in the ground state. The parameters are the same as in Fig. 6. All the spectra are spin neutral.

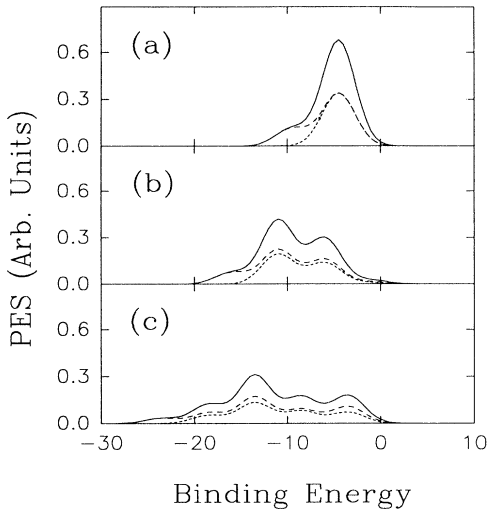

FIG. 8. The calculated photoemission spectrum (PES) with seven electrons in the ground state. The parameters are $t_{dd} = 0.0$, $t_{pp} = 0.5$, $\epsilon = E_p - E_d = 4.0$, $U_d = 5.0$, $U_p = 0.0$, $K = 0.0$, and $t_{dp} = 0.0$ (a), 0.5 (b), and 1.0 (c). See the text for the definition of the parameters. The solid, long-, and short-dashed lines represent the total, majority-, and minority-spin results.

tem, insensitive to details of the single-particle electronic structure.[17]

In previous work[11,15] it was shown that the photoelectron spectroscopy of charge-transfer systems is very sensitive to the hybridization between the "d" and "p" electrons. It is particularly true in the hole-doped case due to a fundamental asymmetry in electron and hole doping in a charge-transfer model away from half-filling, in contrast to the case for the ordinary Hubbard model where an electron-hole symmetry is observed. Here we study a hole-doped charge-transfer system with nonlocal interactions. We still consider the case of seven electrons in the eight-site cluster structure with periodic boundary conditions [see Fig. 1(a)], i.e., an almost-half-filled system. We assign a "d" orbital on each of the sites 1–4 and a "p" orbital on each of the sites 5–8. The Hamiltonian describing the system reads

$$H_{ct} = H + \sum_{i\sigma} E_i c^{\dagger}_{i\sigma} c_{i\sigma}, \tag{12}$$

where the first term H is given by the Hamiltonian (1) with $U_i = U_d$ (U_p) on the "d" ("p") sites, $t_{ij} = t_{dd}, t_{pp}, t_{dp}$ for electron hopping between the sites indicated by the subscripts. $E_i = E_p$ or E_d, depending on the site assignment, are the on-site orbital energies for the "d" or "p" sites.

We have calculated the photoemission and inverse photoemission spectra of the above charge-transfer system. Two sets of parameters have been used to study the effects of the "d"-"p" hybridization and the nonlocal interaction on photoelectron spectroscopy. In the first case, we set $t_{dd} = 0.0$, $t_{pp} = 0.5$, $\epsilon = E_p - E_d = 4.0$, $U_d = 5.0$, $U_p = 0.0$, $K = 0.0$, and the "d"-"p" hybridization parameter is varied with values $t_{dp} = 0.0, 0.5, 1.0$. We then turn on the intersite interaction while keeping all other parameters the same.

The calculated PES and IPES with the first set of parameters are presented in Figs. 8 and 9. The most noticeable effect of the increasing "d"-"p" hybridization is the broadening of the spectra, corresponding to an increase in the single-particle bandwidth. A satellite structure (shoulder) clearly seen in the spectra when $t_{dp} = 0.0$ is significantly reduced when t_{dp} becomes large. The shift of the position(s) of major peaks in the spectra is mainly due to changes in the single-particle electronic structure of the system. Because of the reduced correlation effect, the spin polarization is reduced on the high-energy scale and enhanced on the low-energy scale as t_{dp} increases.

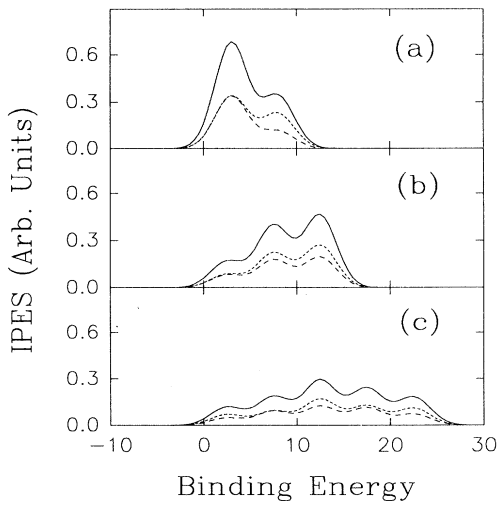

FIG. 9. The calculated inverse photoemission spectrum (IPES) with seven electrons in the ground state. The parameters are the same as in Fig. 8.

When the intersite interaction is turned on, electron hopping between "d" and "p" sites will cost extra energy. It is thus expected that the effect of t_{dp} will be reduced. In Figs. 10 and 11 the calculated PES and IPES for $K = 2.0$ are shown. The results are consistent with the expectation. Compared with the results for $K = 0.0$, a K-driven narrowing in spectral distribution is clearly seen and the spectra are insensitive to changes in t_{dp}. When the value of K is further increased to 5.0, the calculated spectra (not shown here) become essentially independent of t_{dp} as the single-particle electronic structure is dominated by the t_{pp} term in the ground-state configuration. The double-peak structure seen in the IPES is due to the K term as discussed above.

Finally, we study a so-called "negative charge-transfer-energy" system with a negative $\epsilon = E_p - E_d$.[18] We still consider seven electrons in the eight-site periodic cluster. The parameters used in the calculation are the same as in the above "positive charge-transfer-energy" case (Figs. 8 and 9), except here $\epsilon = -3.0$ and a larger range for t_{dp} (up to 2.0) is used. We first look at the $K = 0$ case. The calculated spectra are shown in Figs. 12 and 13. It should be noticed that with these parameters a typical ground-state configuration consists of paired-electron states, similar to the situation in the large-K case, but for a different reason. Here ($K = 0.0$) it is due to the fact that $U_{pp} = 0.0$ and ϵ is negative. Therefore the configuration with pairs of electrons on the "p" orbitals (i.e., sites 5–8) is energetically favorable. The hybridization term t_{dp} broadens the spectral distribution similar to the results shown above for the positive charge-transfer-energy system. Compared with the results in Figs. 8 and 9, it is seen that the spectra are less sensitive to the change in t_{dp} here. This is because the electrons are less mobile due to the negative charge-transfer energy which tends to pair ("trap") the electrons on the "p" sites as discussed above. In this sense a negative charge-transfer-energy system behaves like a large-K system with positive charge-transfer energy.

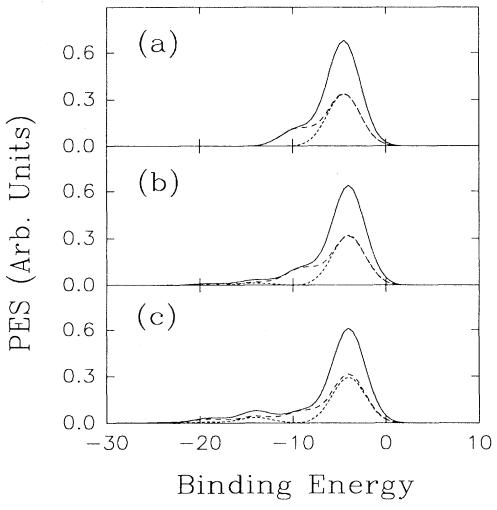

FIG. 10. The calculated photoemission spectrum (PES) with seven electrons in the ground state. The parameters are the same as in Fig. 8, except here $K = 2.0$. The solid, long-, and short-dashed lines represent the total, majority-, and minority-spin results.

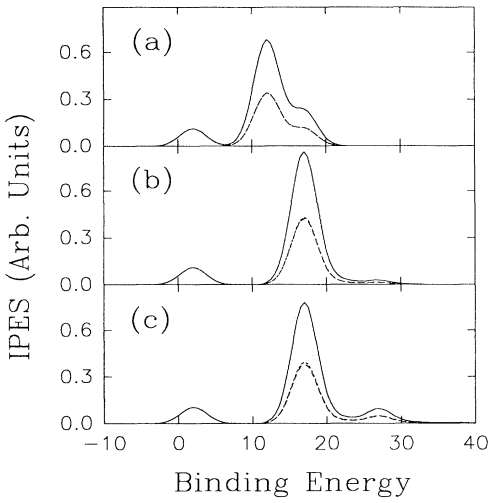

FIG. 11. The calculated inverse photoemission spectrum (IPES) with seven electrons in the ground state. The parameters are the same as in Fig. 10.

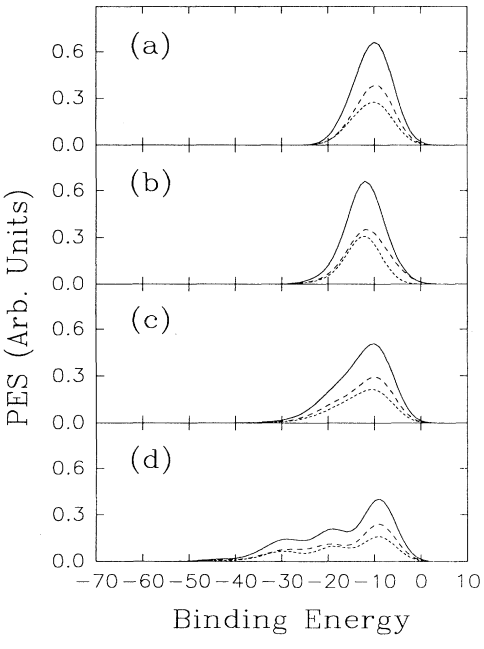

FIG. 12. The calculated photoemission spectrum (PES) with seven electrons in the ground state. The parameters are the same as in Fig. 8, except here $t_{dp} = 0.0$ (a), 0.5 (b), 1.5 (c), 2.0 (d), and $\epsilon = -3.0$.

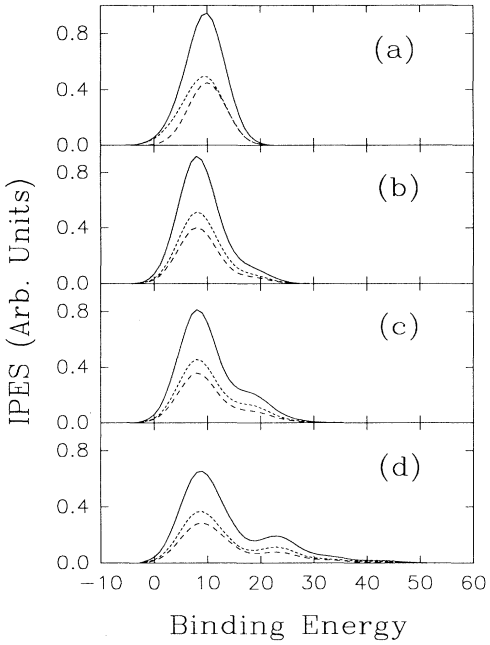

FIG. 13. The calculated inverse photoemission spectrum (IPES) with seven electrons in the ground state. The parameters are the same as in Fig. 12.

When the intersite interaction K is turned on, the ground-state pairing ("trapping") effect is further enhanced and the electrons will essentially be localized, since hopping to a "d" orbital is very costly in energy. As a result, the spectra should be distributed in a narrower range in energy due to the effect of the K term and

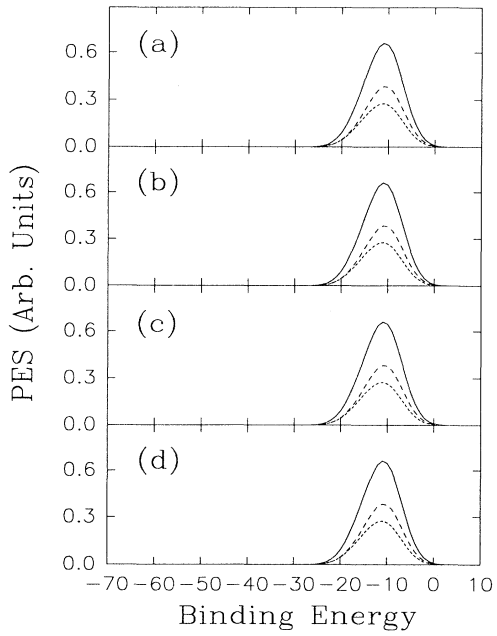

FIG. 14. The calculated photoemission spectrum (PES) with seven electrons in the ground state. The parameters are the same as in Fig. 12, except here $K = 5.0$.

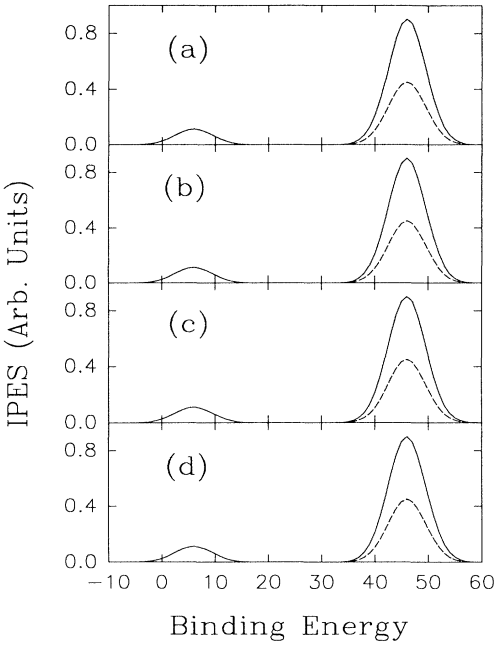

FIG. 15. The calculated inverse photoemission spectrum (IPES) with seven electrons in the ground state. The parameters are the same as in Fig. 14.

be essentially independent of t_{dp}. This is indeed the case in the calculated photoemission and inverse photoemission spectra as shown in Figs. 14 and 15. A two-peak structure is seen in the IPES. This is the manifestation of the paired ground-state configuration driven by the large K and further enhanced by the negative value of ϵ as discussed above. A simple analysis determines that the energy separation between the two peaks should be $7K - \epsilon$. It equals 38.0 with the chosen parameters $K = 5.0$ and $\epsilon = -3.0$, which is in excellent agreement with the calculated results shown in Fig. 15.

IV. CONCLUSIONS

We have examined the effect of nonlocal interactions on the photoemission and inverse photoemission spectral distribution in an extended Hubbard model. By adjusting the Hamiltonian parameters, two different systems are studied: the first is a uniform Hubbard system and the other is a two-sublattice charge-transfer system.

In the case of the Hubbard system, it is found that the intersite interactions generally suppress the features driven by the on-site interaction and lead to an overall narrowing in the spectral distribution. In the photoemission spectrum, the spectral weight driven by the on-site interaction U is pushed by the intersite interaction K toward the lower-energy side and the U-driven effects manifest themselves near the chemical potential in the large-K limit, which is opposite to the case of an ordinary Hubbard model with $K = 0$. In the inverse

photoemission spectrum, a peak that grows linearly in weight with the doping concentration is observed. Its spin polarization develops from fully polarized to neutral as the system is doped away from half-filling. These behaviors are qualitatively different from those of an ordinary Hubbard system or a semiconductor or a simple metal system.

In the case of the charge-transfer system, the hybridization (with hopping parameter t_{dp}) between the strongly correlated "d" electrons and uncorrelated "p" electrons broadens the spectral distribution in the absence of the intersite interaction K, as expected from a single-particle analysis. When K is large the effect of the "d"-"p" hybridization on the spectra is greatly reduced and the effect of the K term becomes dominant. A smooth transition between these two regimes is expected. The effect of K is more significant in a negative charge-transfer-energy system than in a positive charge-transfer-energy system since the negative charge-transfer energy causes pairing of electrons on the "p" sites. In this sense, the effect of this negative energy difference between the "p" and "d" orbitals is equivalent to that of an effective K, although a true K term does not discriminate "d" or "p" sites in terms of pairing electrons in the ground-state configuration.

The calculated results are analyzed in a many-body picture to gain physical insights into the nature of the many-body states and the fundamental roles of the nonlocal interaction in determining the spectroscopic behavior. Although some results have been discussed in the limit of large nonlocal interactions to help understand the underlying physics, most effects already can been seen for moderate or even small interactions, as demonstrated in the reported calculations. The qualitative physics presented in this work is expected to have general implications for a wide variety of strongly correlated systems with appreciable nonlocal interactions.

ACKNOWLEDGMENTS

We acknowledge helpful discussions with Tao Pang, Ki Ho Lee, and Jianbo Zhang. J.Z. was partially supported by the Graduate College of the University of Nevada, Las Vegas (UNLV) through a Graduate Assistantship. This work was supported in part by the National Science Foundation under Cooperative Agreement OSR-9353227 and the U.S. Department of Energy under the EPSCoR program. Part of the numerical calculation was carried out on the Cray YMP at the National Supercomputing Center for Energy and the Environment at UNLV.

[1] For a recent review, see J. W. Allen, *The International Conference on Strongly Correlated Electron Systems, Amsterdam, 1994* [Physica B (to be published)].

[2] Z. X. Shen, W. E. Spicer, D. S. Dessau, D. M. King, and B. O. Wells, Science **267**, 343 (1995), and the references cited therein.

[3] It should be noted that most experimental data show that the density of initial states only describes the photoemission spectra for photon energies in the soft-x-ray range, or for polycrystalline materials. One should be careful in relating theoretical results to photoemission spectra.

[4] For a recent review, see E. Dagotto, Rev. Mod. Phys. **66**, 763 (1994), and references cited therein.

[5] C. Guillot *et al.*, Phys. Rev. Lett. **39**, 1632 (1977); D. E. Eastman *et al.*, *ibid.* **40**, 1514 (1978); F. J. Himpsel *et al.*, Phys. Rev. B **19**, 2919 (1979); L. A. Feldkamp and L. C. Davis, Phys. Rev. Lett. **43**, 151 (1979); W. Eberhardt and E. W. Plummer, Phys. Rev. B **21**, 3245 (1980); R. Clauberg *et al.*, Phys. Rev. Lett. **47**, 1314 (1981).

[6] D. R. Penn, Phys. Rev. Lett. **42**, 921 (1979); A. Liebsch, *ibid.* **43**, 1431 (1979); N. Martensson and B. Johansson, *ibid.* **45**, 482 (1980); L. C. Davis and L. A. Feldkamp, Solid State Commun. **34**, 141 (1980); L. Kleinman and K. Mednick, Phys. Rev. B **24**, 6880 (1981); R. Clauberg, *ibid.* **28**, 2561 (1983); R. H. Victora and L. M. Falicov, Phys. Rev. Lett. **55**, 1140 (1985).

[7] Changfeng Chen, Phys. Rev. Lett. **64**, 2176 (1990); J. Phys. Condens. Matter **4**, 9855 (1992); Phys. Rev. B **45**, 13 811 (1992); **48**, 1318 (1993).

[8] S. R. White and R. M. Noack, Phys. Rev. Lett. **68**, 3487 (1992); S. R. White, Phys. Rev. B **48**, 10 345 (1993).

[9] Changfeng Chen, Int. J. Mod. Phys. B **5**, 1147 (1991); J. K. Freericks and L. M. Falicov, Phys. Rev. B **42**, 4960 (1990).

[10] A. Moreo and E. Dagotto, Phys. Rev. B **42**, 4786 (1990); H. J. Schmidt and Y. Kuramoto, *ibid.* **42**, 2562 (1990); E. R. Gagliano, C. A. Balseiro, and M. Avignon, Europhys. Lett. **12**, 259 (1990).

[11] H. Eskes, M. B. Meinders, and G. A. Sawatzky, Phys. Rev. Lett. **67**, 1035 (1991).

[12] E. Dagotto, R. Joynt, A. Moreo, S. Bacci, and E. Gagliano, Phys. Rev. B **41**, 9049 (1990).

[13] M. Tinkham, *Group Theory and Quantum Mechanics* (McGraw-Hill, New York, 1964); A. W. Luehrmann, Adv. Phys. **17**, 1 (1968).

[14] L. Tan, Q. Li, and J. Callaway, Phys. Rev. B **44**, 341 (1991); J. Callaway, J. W. Kim, L. Tan, and H. Q. Lin, *ibid.* **48**, 11 545 (1993); J. Callaway, L. Tan, and H. Zheng, *ibid.* **50**, 1369 (1994).

[15] L. F. Feiner, Phys. Rev. B **48**, 16 857 (1993).

[16] To illustrate the qualitative physics we can use a dimer model with one electron in the atomic limit. It is easy to find that the energy separation similarly defined as in the PES case is $\Delta = U - K$, which decreases with increasing K.

[17] This shows that the spectral features driven by nonlocal interactions are quite robust. However, photoelectron spectra are usually sensitive to, and sometimes even dominated by, the single-particle electronic structure if photon energies are below 60 eV [see, e.g., R. Clauberg, E. M. Haines, and R. Feder, Z. Phys. B **62**, 31 (1985)].

[18] T. Mizokawa, H. Namatame, A. Fujimori, K. Akeyama, H. Kondoh, H. Kuroda, and N. Kosugi, Phys. Rev. Lett. **67**, 1638 (1991).